

Single-step-model analysis of angle-resolved photoemission from Ni(110) and Cu(100)

D. W. Jepsen, F. J. Himpsel, and D. E. Eastman

IBM T. J. Watson Research Center, Yorktown Heights, New York 10598

(Received 15 January 1982)

Detailed computer calculations of angle-resolved photoemission are used to demonstrate that experimental data on Ni(110) and Cu(100) show effects that are found in the single-step model of photoemission, but not contained in the usual three-step model. In particular, the effect of inelastic scattering on the widths and shapes of direct-transition peaks is investigated directly and compared with simple line-shape formulas which are derived from the theory. Constant-initial-state spectra provide a particularly useful method for the determination of the inelastic scattering in the upper state. However, direct interpretation by a Lorentz-curve fit may overestimate the inelastic scattering slightly, since a somewhat smaller value is obtained by comparing the experiment with detailed calculations. Proper interpretation of the nickel data requires that the upper-state bands should be calculated including a damping due to inelastic scattering. Surface-matching effects appear to influence the shape of direct-transition peaks in copper.

I. INTRODUCTION

In this paper we examine, by detailed computer calculation, some of the effects contained in a single-step model of photoemission which are not contained in the usual three-step model, and demonstrate that they occur in previously published experimental data on Ni(110) (Ref. 1) and Cu(100).^{2,3} In the usual three-step model of the photoemission experiment, the observed phenomenon is simplified by breaking it up into three separate processes: (1) The transition of electrons from an initial state below the Fermi level to a final state in the bulk of the crystal at the energy at which they are later collected, (2) transport of these excited electrons from the bulk of the crystal to the surface with attenuation of the flow due to inelastic scattering, and (3) transmission of these electrons from the crystal to the detector in vacuum with a loss due to (possibly total) internal reflection. This model has been compared quite successfully with experimental data.⁴ However, in this model there is no photoemission when there is no final-state Bloch wave with a k vector equal to the k vector of one of the possible initial-state Bloch waves. (We assume here that the wave vector of the photon is negligible.) This aspect of the model limits it to direct transitions, and, because of the exact conservation of k , it does not deal with the width of direct transition lines.

In the more sophisticated single-step model of photoemission these three steps are combined into a single coherent quantum process. Surface photoemission is contained in the single-step model, and

this emission is clearly not contained in the three-step model. However, in this paper we limit ourselves to an increased understanding of the bulk emission that can be obtained by going from the three-step model to the single-step model.

In particular, we note that in the three-step model the excitation of an electron from the initial state to the final state is a bulk transition between the energy bands of the solid. In the single-step model this excitation process is modified by the inelastic scattering, as well as the presence of the surface. In the three-step model, the inelastic scattering and surface effects cannot influence the excitation process because they are relegated to separate, later steps. One result of combining the steps is that the Bloch wave functions and band energies to be compared with photoemission experiments (particularly the upper-state wave functions) should be calculated including inelastic scattering. This has already been pointed out by Nilsson and Dahlbäck,⁵ and by others,⁶ the earliest relevant work probably being that of Slater.⁷ We have substantiated, by detailed calculations for nickel, the effects of wave damping proposed by Nilsson and Dahlbäck on the basis of simple-model calculations for copper.

We find that peak widths are largely determined by the inelastic scattering, although density-of-states effects also play a role. We derive simple expressions for the shapes and linewidths of direct transition peaks from the single-step model and compare these results with more detailed computer calculations and with experimental data.

We also focus on the problem of finding the life-

time of an electron in the upper state from photoemission experiments. We compare the published experiments on Ni(110) and Cu(100) with detailed calculations to determine the lifetimes implied by these experiments. Using the analysis, we then assess the validity of using simple linewidth formulas for finding lifetimes. In particular, one can also obtain the inelastic scattering in the upper state quite directly from the widths of direct transition peaks in experiments in which the collection energy and photon energy are varied together so that the initial-state energy remains constant. If a suitable initial state can be found, this indeed appears to give a relatively simple method for obtaining the inelastic scattering,^{2,3,8} although comparison with the procedure using detailed calculation of the photoemission indicates that this simpler method may overestimate the amount of inelastic scattering.

The photoemission in a gap in the band structure should be less attenuated by inelastic scattering than photoemission into bulk band states. Comparing photoemission in a gap with the photoemission into a nearby band should give a measure of the inelastic scattering in the band without an absolute calibration of the signal into the detector. We use detailed calculations to extract the inelastic scattering from this comparison. This procedure gives a result which agrees generally with the results we obtain from peak widths, but, at present, does not appear to be more accurate than the peak-width results.

We also demonstrate here, using the Ni(110) data, that such photoemission in a gap can have a definite bulk character, in the sense that, when we take the inelastic damping into account, it occurs between the same initial and final Bloch waves as ordinary bulk emission, and that these waves are not changed qualitatively in character. The usual direct-transition peaks can occur even when the upper-state electron has a quite short mean free path, in fact only four layers of penetration are sufficient.⁹ Thus it is not surprising that bulk emission persists in a gap, where the upper state is only somewhat more strongly decaying than in a band. To understand the k_z values actually involved in such transitions, it is necessary to take into account the effect of inelastic scattering on the band structure.

II. THEORY OF ABSORPTION EFFECTS, DERIVATION OF SIMPLE LINE-SHAPE FORMULAS

The theoretical treatment used in this work is based on a rigorous description of the effects of in-

elastic scattering, and treats them in a particularly lucid way. In a many-body treatment of the motion of an electron through the crystal, these effects are produced by the imaginary part of the self-energy in the equation for the single-particle Green's function. This imaginary part acts like an absorptive term in the potential. In the present work, the upper-state band structure of the crystal is calculated with the imaginary part of this self-energy term included with the potential. The calculated Bloch waves have wave vectors with a positive imaginary part in the direction of the energy flux, and hence their amplitudes decay as they move through the crystal.

As is common in low-energy electron diffraction (LEED) calculations,¹⁰ the imaginary part of the self-energy, $-\beta$, is taken to be independent of the position and direction of motion of the electron, but may depend on its energy. Following Slater⁷ we will call β the damping, and also sometimes the absorption. Adding this negative imaginary term to the potential is equivalent to adding the imaginary term $i\beta$ to the energy.

A simple description of the line shape can be obtained directly from this addition of an imaginary term to the energy. According to the time-dependent Schrödinger equation

$$(E_0 + i\beta)\psi = i\hbar \frac{\partial \psi}{\partial t}, \quad (1)$$

the final-state wave function in the photoemission process must decay exponentially with time. Fourier transform from time to frequency then suggests that the line shape for the transition will be Lorentzian.¹¹ We shall not pursue this further because the standard treatments of the single-step model, which give a more complete picture of the various factors which can influence line shape can be developed directly from a time-independent steady-state scattering theory.

In the single-step model, the imaginary part of the wave vector κ of a Bloch state which is obtained from

$$E(k_x, k_y, k_z + i\kappa) = E_0 + i\beta \quad (2)$$

plays a much more direct role in determining the line shape than β . The quantities k_x , k_y , and E_0 are determined by the geometry and collection energy of the experiment. For a uniform imaginary contribution to the potential β , the procedures of our computer program are equivalent to solving this implicit equation. This κ is easily related to a mean free path for an electron (or hole if we look at the lower-state bands) in the final state of the electronic

transition. Since this mean free path measures the loss of coherence of the wave rather than the electron's loss of momentum, it is more directly related to the lifetime of the state than to the mean free path measured in the usual layer-penetration experiments,¹² in which the attenuation of emitted electrons is studied using absorbed layers of varying thicknesses. Phonon or electron scattering near the forward direction has little effect in such experiments, but is completely effective in destroying phase coherence. One would expect that this κ would show greater spatial variation and directional anisotropy than the experimentally measured mean free path. Such effects may be obtainable from the interpretation of photoemission data sufficiently resolved in energy and angle, and would give valuable information about the self-energy of excited electrons (and holes) in the crystal.

We have some idea of the value to be expected for β from LEED analyses,¹⁰ which find agreement between theory and experiment for typical materials with values of β around 3 to 4.5 eV for electrons with kinetic energies from 30 to 150 eV. Similar values are obtained from calculations for a uniform electron gas.¹³ There are also inelastic processes in LEED involving phonons which leads to a Debye-Waller factor that gives a smooth decrease in intensities with increasing energy. Although Debye-Waller effects have been included in photoemission calculations,¹⁴ it is probably better, at room temperature and below, *not* to include them in the usual simple form. This is because Eq. (3), the theoretical expression from which we obtain the photoemission gives only the intensity of electrons which suffer no inelastic scattering in leaving the crystal. Thus if the Debye-Waller factor is included, electrons which are scattered through some angle by a phonon on its way out of the crystal are treated as totally lost. Since many of these phonon-scattered electrons are deflected through only small angles and leave the crystal with a negligible loss of energy, they will be detected as though they were elastic electrons. We can include these electrons in the calculation by leaving out the Debye-Waller factor and treating them as elastic electrons. This will be a good approximation as long as the phonon scattering is primarily near the forward direction. Of course, when most of the phonon scattering is away from the forward direction, it is better to put the Debye-Waller factor in. At high temperatures and high energies, where phonon scattering is strong and not restricted to the forward direction, the experimental photoemission is best described by the indirect transition model.¹⁵

The single-step model gives a general description of the photoemission process which reduces to a direct-transition description under appropriate circumstances.¹⁶ If we disregard emission from the surface itself, the intensity of emitted electrons has the form^{9,16}

$$I \propto \left| \sum_m \sum_n C_n^* C_m \Delta(n, m) \langle n | \vec{p} \cdot \vec{E} | m \rangle \right|^2 \quad (3)$$

with

$$\Delta(n, m) = \frac{1}{\exp[(ik_z^{nf*} - ik_z^{mi} - \lambda)\alpha] - 1}, \quad (4)$$

where C_m and C_n are the coefficients of the Bloch waves m and n in the initial and final states, respectively, and where $\langle n | \vec{p} \cdot \vec{E} | m \rangle$ is the matrix element of the electric field between these states evaluated for a single bulk cell.

Direct-transition behavior is produced by the interference of the waves emitted from different planes of the crystal parallel to the surface. The factor Δ of Eq. (4) arises from summing the contributions of all the layers of the crystal parallel to the surface. These contributions from the various layers differ only by powers of the exponential factor in the denominator of Δ . We obtain simplified formulas for the line shape of a direct transition by simplifying Δ . Here a is the length of the unit cell perpendicular to the surface, $\exp(-\lambda a)$ is the decrease of the electric field in penetrating one layer, and k^i and k^f are the wave vectors of the initial and final Bloch waves. The decay of the electric field is generally small, so that λ can be set equal to zero in discussing the properties of this expression.

Direct transitions occur when $\Delta k = k_z^f - k_z^i$ is small in one of the terms, i.e., when the final and initial wave are in phase on all the planes of the crystal below the plane of the surface. When this is true, the denominator of Δ in this term is near zero. We need consider only this one large term in the sums in this case. The denominator cannot reach zero because k^f has the imaginary part κ^f , due to inelastic electron scattering, and k^i has the imaginary part κ^i due to inelastic scattering, γ (analogous to β), of the hole. Because of both of these imaginary parts, the contributions from deeper layers are reduced, and the interference between layers responsible for the direct-transition selection rule is also reduced.

When the inelastic scattering is small, we may expand the absolute square of the factor in Eq. (2) to second order in Δk (around the position of a direct transition) to obtain the result

$$|\Delta|^2 = \frac{1}{(k_f^i - k_r^i)^2 + (\kappa^f + \kappa^i)^2}. \quad (5)$$

Here k_f has been written for the real part of k_z . Because the final state is a *time-reversed* LEED wave function, the imaginary parts of the final and initial k 's add although the real parts subtract. The expansion used here is valid if $\Delta k \alpha \ll 1$, i.e., if the transition is localized to a small region of the Brillouin zone. This must be fulfilled in any experiment in which the bands can be mapped out.

One usually measures the variation of the emission intensity with energy, either the energy of the outgoing electron or the photon energy. In the neighborhood of a direct transition this variation arises from the variation of the k 's in Eq. (5). We shall study two cases. First, when the photon energy and collection energy are varied together so that the initial energy (and k^i) is constant (the so-called constant-initial-state spectrum, such as in Refs. 2 and 3), and second, when the collection energy is varied at constant photon energy so that both the initial and final states change (the so-called energy distribution curve) such as in Ref. 1. The quantities which determine the peak widths are found to be different in these two cases. We may convert the variation of this expression with k to a variation with collection energy in an approximate way by performing a Taylor expansion of Eq. (2) for the initial and final states. If we expand Δk about zero which is the position of direct transition, we obtain

$$|\Delta|^2 = \frac{A^2}{(\Delta E)^2 + (\kappa^f + \kappa^i)^2 A^2}, \quad (6a)$$

with

$$A^{-1} = \frac{\partial k_z^i}{\partial E} - \frac{\partial k_z^f}{\partial E} = \left[\frac{\partial E^i}{\partial k_z} \right]^{-1} - \left[\frac{\partial E^f}{\partial k_z} \right]^{-1} \quad (6b)$$

or

$$A = \frac{\partial E^f}{\partial k_z} \frac{\partial E^i}{\partial k_z} \left[\frac{\partial E^f}{\partial k_z} - \frac{\partial E^i}{\partial k_z} \right]^{-1} \quad (7)$$

when the photon energy is constant, and

$$A = \frac{\partial E^f}{\partial k_z} \quad (8)$$

when the initial energy is constant. Furthermore, if the inelastic scattering, β , of the electron is small, we have by a Taylor expansion of Eq. (2),

$$\kappa^f \frac{\partial E^f}{\partial k_z} \cong \beta. \quad (9)$$

This approximation is nearly exact for quadratic

bands because the κ^2 term is real, and therefore does not contribute to the imaginary term containing β . If the hole lifetime is long we have the same approximation for κ^i ,

$$\kappa^i \frac{\partial E^i}{\partial k_z} \cong \gamma. \quad (10)$$

Thus, Eq. (6) becomes

$$|\Delta|^2 = \frac{A^2}{(\Delta E)^2 + (\gamma + \delta)^2}, \quad (11)$$

where

$$\delta = (\beta + \gamma) \frac{\partial E^i}{\partial k_z} \left[\frac{\partial E^f}{\partial k_z} - \frac{\partial E^i}{\partial k_z} \right]^{-1}$$

in the case when the photon energy is held constant, and

$$|\Delta|^2 = \frac{A^2}{(\Delta E)^2 + (\beta + \zeta)^2}, \quad (12)$$

where

$$\zeta = \gamma \frac{\partial E^f}{\partial k_z} / \frac{\partial E^i}{\partial k_z}$$

when the initial state is held constant. Both of these expressions give the standard Lorentzian line shape if we assume that β, δ, ζ , and the other factors in the intensity are constant across the peak profile. We see that the approximations necessary to obtain a Lorentzian shape are not severe. However, we do find deviations. In the work on nickel we find that the density of states can vary across the peak. In the work on copper we find that there are deviations from Lorentzian shape which arise because other terms in Eq. (3) beside the dominant, direct-transition term are not completely negligible.

The matrix element over a bulk cell can also vary across the line, but this shows the same behavior as we have just found for Δ . This is to be expected because the interference between the scattering from different atomic layers we have described extends to interference between the scattering from different planes within an atomic cell. This is particularly clear when the initial and the final Bloch waves are represented by plane waves. In this case the interference within cells and between cells can be treated on the same footing. If the initial Bloch wave is better represented by a tight-binding form with wave functions localized on the atoms, and the transition occurs principally to a single spherical-harmonic component of the final state (as is often the case), the interference effects within the cell will be small.

III. DISCUSSION OF THE NICKEL DATA

In the usual determination of the lower-state bands using photoemission, the energy of the initial state and the component of its k vector in the plane of the surface are easily obtained from the parameters of the experiment but the determination of the value of k_z , the component of the wave vector perpendicular to the surface, is more difficult. Usually, k_z is obtained from knowledge of the upper state of the transition which, according to the direct-transition model, has the same value of k_z . This upper state is normally approximated by a nearly-free-electron model adjusted to fit the gaps and critical points observed in the experiment. When the energy of the upper state reaches a gap in the band structure, in a simple description without damping, one expects the peak to disappear for lack of a final state.

In the experimental data for normal emission from Ni(011) the observed peaks do not disappear beyond a band edge, but become stationary with photon energy. Figure 1 shows the previously published¹ electron emission as a function of lower-state energy for a sequence of photon energies. These were taken at constant instrumental energy resolution and aperture so that the intensity of

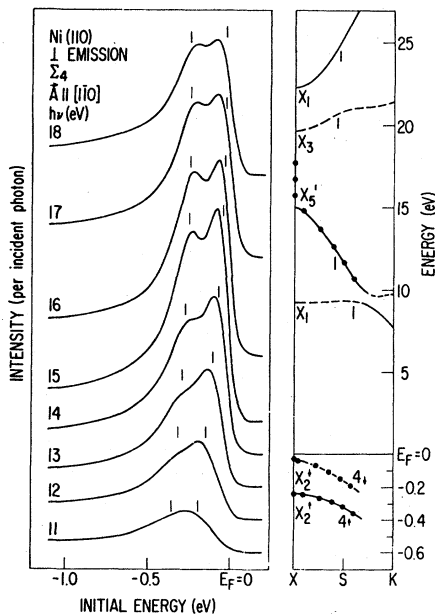


FIG. 1. Normal photoemission from Ni(110). To the left are experimental energy distribution curves for a number of photon energies. To the right, the upper-state bands used in interpreting these spectra, and the lower-state bands obtained from this data (from Ref. 1).

emission observed for different photon energies can be compared directly on the same scale. The results were obtained for s -polarized light (electric field parallel to the surface) with the consequence that no plasmon or other dielectric effects,⁴ and no surface photoemission, are involved in their interpretation.

We see that there is an unresolved pair of peaks at -0.35 and -0.19 eV at 11 eV photon energy (marked by ticks), which move up with photon energy to -0.25 and -0.04 eV at 15 eV photon energy. The tick-marked peak positions were obtained by resolving the experimental structure into two Lorentzians of equal area but differing widths and a steplike electron-loss function for the secondary electron background.¹ As the photon energy increases from 16 to 18 eV, the peaks remain at the same initial-state energy of -0.24 and -0.03 eV. Below the photon energy of 15 eV, this pair of peaks has been determined to be direct emission from the spin-split s - p bands along the S line (K to X) in the Brillouin zone to an upper state which comes into X_5 , as shown at the right side of Fig. 1. Above 15 eV, we find that these same peaks, now stationary, correspond to transitions to the LEED wave function in a gap in the band structure [originally determined by comparison with Cu(011)].¹⁷

The intensity of these peaks increases as the photon energy increases from 11 to 15 eV, as one might expect from the increase of the initial density of states as the transition moves along the band towards the flat region around the X point. For photon energies above 15 eV the strengths of these peaks decrease to about 95% of their maximum values at 16 eV photon energy, and 65% at 18 eV. Such a decline is expected from the increased attenuation of the evanescent waves from the surface of the crystal as the upper-state energy of the transition moves deeper into the gap, and the LEED wave function is more strongly attenuated. Note, however, that at 18 eV, which is near the middle of the calculated gap, the strength of these peaks is still greater than the strength of these same pair of peaks at 13 eV, where they represent "standard" direct transitions into a normal bulk Bloch state.

IV. COMPARISON OF THEORY WITH THE NICKEL EXPERIMENTS

The computer program used in this work is described in previous publications.^{9,18} Briefly, the photoemission is calculated as a transition from the initial state representing the reflection of a bulk Bloch wave at the surface to a final state given by

the time-reversed LEED wave function with inelastic scattering taken into account as discussed in Sec. II. The initial state contains not only the incoming and reflected Bloch waves, but also the evanescent waves in the neighborhood of the surface required to match with the proper exponential tails in vacuum. The final state is also composed of Bloch waves, here carrying flux towards the surface and also evanescent waves in the surface region. For emission in a gap, all of the waves present in the final-state wave function are evanescent. When there is more than one band at the initial energy, we add together the photoemission intensities from the separate initial states, each made up from a Bloch wave moving toward the surface and its reflected waves.

The photoemission calculations were performed by a "beam" method¹⁹ which is quite standard in LEED work. This method of calculation becomes more difficult when the planes of atoms parallel to the surface of the crystal are close together relative to the spacing of the atoms within a plane. We find for the Ni(110) surface that 41 Fourier coefficients were necessary to obtain an adequate representation of the initial-state wave functions halfway between the planes of atoms. This was far more than were needed for the upper state, and also far more than were needed in previous calculations for Cu(001) and Cu(111).¹⁸

The hole lifetime τ has been set equal to zero in the calculations presented here for nickel, because the initial state involved in these experiments is very close to the Fermi level. Hence, the shapes of the computed peaks are determined by β , and by the changing slope of the initial band which gives the variation of the initial density of states. Note that various approximations have been used in the derivations of Eq. (11). The computer program used in this work evaluates Eq. (3) directly without these approximations. As a result, the actual computed line shape does differ from a simple Lorentzian. Our calculations do in fact give line shapes and widths quite close to what is seen experimentally. Examination of the calculations shows that the difference in shape that we calculate from the simple form arises from the change in the initial density of states with energy. In particular, the spectral peak is cut below the Fermi level because of a lack of available initial band states.

Figure 2 shows photoemission intensity curves calculated for the values 1.75 and 2.5 eV of the imaginary contribution to the potential used to obtain the upper-state wave function in the photoemission process. These are to be compared with the experi-

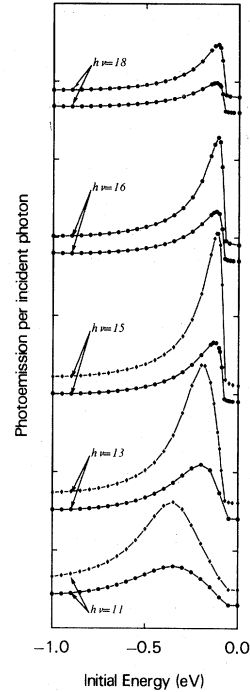


FIG. 2. Photoemission from Ni(110) as calculated in this work. Upper curve of each of these pairs of curves is calculated for an absorption of 1.75 eV, and the lower curve for an absorption of 2.5 eV. It is estimated that the actual experimental absorption of the upper-star electrons is between these values, perhaps nearer the lower value since these curves are not broadened to simulate experimental energy resolution.

mental curves of Fig. 1. Calculations were performed for paramagnetic rather than ferromagnetic nickel so that a single degenerate spin peak in the theory must be compared with the spin-split pair in the experiment. The potential used was that of Moruzzi, Janak, and Williams.²⁰ The behavior of the photoemission intensity with the change in character of the upper state between band and gap should be modeled adequately by these calculations for paramagnetic nickel. The calculated peak shapes compare quite well with either of the spin-split pair in the experiment and the trend in changing peak heights with photon energy is reproduced qualitatively.

Comparing the 1.7- and 2.5-eV absorption curves, we see, as might be expected, that the effect of increasing the inelastic scattering in the upper state is to reduce the intensity of photoemission everywhere, but most strongly in the region below 15-eV photon energy where the emission arises from transition to a final state containing bulk Bloch waves for which band-gap effects do not limit the penetra-

tion of the final-state wave function into the solid. From a comparison of the two sets of theoretical curves with the experimental curves, our best estimate of the damping β is between 1.75 and 2.5 eV, i.e., about 2 eV. The calculated peaks have not been broadened to model the resolution of the experimental apparatus, so that perhaps a slightly smaller value of β , e.g., 1.75 eV, is probably more appropriate. Notice that each theoretical peak has a long tail to deeper energy resembling an inelastic tail. This is an *elastic* rather than an inelastic contribution to the photoemission arising from the large value of β , much larger than the peak widths seen here. Inelastic contributions, i.e., scattered secondary electrons are not included in these calculations.

The intensity of the photoemission peaks should be some measure of the volume in the crystal contributing to the observed signal, and hence a measure of the damping which determines the size of this volume. While the absolute intensity of the signal is not easy to measure, one can compare the intensity in a band with the intensity in a nearby gap. The thickness of the region under the surface providing electrons is limited by both known gap-wave effects and inelastic damping for final states in a gap, and only by inelastic damping for final states in a band. Hence, one has the chance of obtaining the inelastic attenuation by comparing the intensity of the photoemission into a band, where it acts alone, with the intensity in the gap, where its action is combined with the known gap-wave effects. We shall attempt to find a damping β which gives the same value of this ratio in our computer calculations as is found experimentally.

To make this comparison we graph, in Fig. 3, the area of the experimental peak structure (including both spin-up and spin-down peaks) compared with the calculated peak areas for photon energies across the region from the band into the gap. The normalization of each of the curves was chosen to give the same area at its maximum, which occurs at 14 eV for the theoretical curves and at 15 eV for the experimental curve. The results shown for various values of the inelastic scattering in the upper state approximate the experimental curve in the gap region above 15 eV, but lie well above the experiment in the band region below 15 eV, for this choice of normalization. Including hole-lifetime effects in the calculation would be expected to reduce rather than improve this aspect of the comparison. The areas actually plotted in this figure are the areas above a straight line drawn tangent to the curve in the tail region around -1.0 eV, because this is a sensible procedure for making the result for the

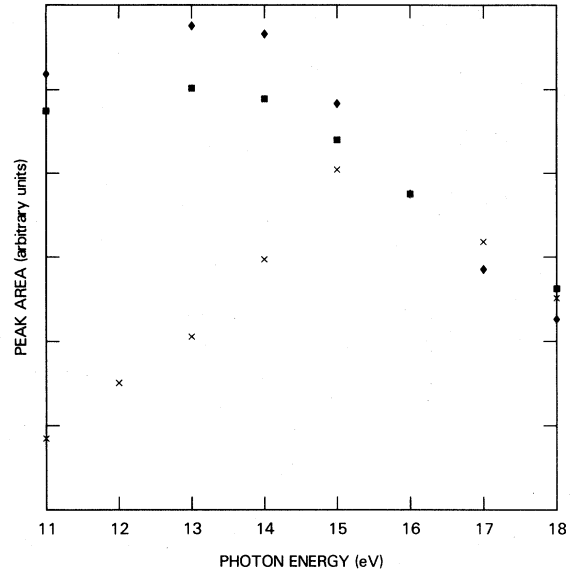


FIG. 3. Areas of the theoretical and experimental peaks above the tail (see text) at various photon energies. \times , experiment; \blacklozenge , theory with an absorption $\beta=1.75$ eV; and \blacksquare , theory with an absorption $\beta=2.5$ eV.

theoretical curves insensitive to the tail region. Integrating the full area of the experimental curves down to this same energy gave essentially the same results. Using peak heights, rather than areas, also gives curves very similar to the ones shown above for the areas, although the problem appears to be that the tails of the theoretical curves are larger than what is seen experimentally.

One would expect that the estimate of the damping which we obtain by comparing the penetration in a band with the penetration in a nearby gap would be less dependent on initial-state lifetime, interference from other peaks, and experimental energy and angle resolution than the result from peak width measurements. Unfortunately, as we see, the theory is presently unable to fit the experimental intensities well enough at present.

V. CALCULATION OF THE DAMPED WAVES IN THE CRYSTAL

The left panel of Fig. 4 shows the upper-state band of principal importance in the photoemission process, calculated with a damping of 1.75 eV as a thin line, and, with no absorption as a series of dots. We plot the energy against the real part of k_z for the plot with absorption. The band moves up the left-hand side of this diagram reaching X at about 17.5 eV. There is a large band gap in the bands

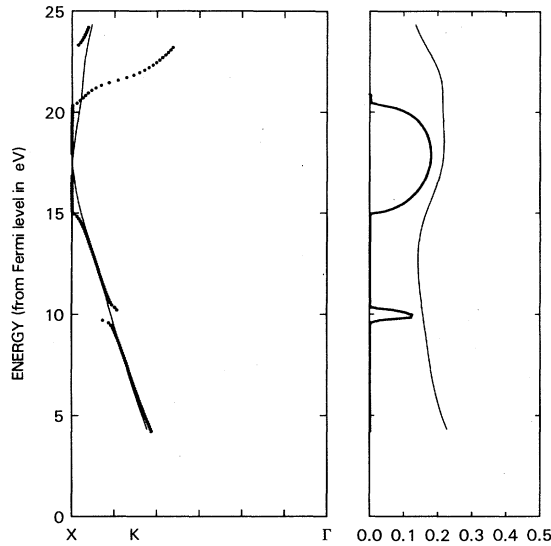


FIG. 4. Band structure along the Γ -K-X direction, perpendicular to the Ni(110) surface. Bands without, and with, 1.75 eV of absorption are plotted on the left with dots and solid line, respectively. The corresponding imaginary part of k_z in inverse angstroms is plotted on the right, a heavy curve for the calculation without absorption, and a lighter curve for the calculations with an absorption of $\beta=1.75$ eV.

without absorption between 15 and 20 eV. This gap is smoothed out in the curve for 1.75-eV absorption. This modification of the band structure by damping is the same behavior as seen in model calculations by Nilsson and Dahlbäck.⁵ There is also a small gap around 10 eV with a flat band which is not shown completely. This gap is also removed by adding absorption. The parts of the bands across the gaps are derived from the real lines which occur in these gaps for the band structure without damping. The transition from a real line to a spanning line can be followed by performing calculations with small amounts of damping.

A comparison of these curves shows that the zero-absorption band structure is a good guide to the band structure obtained with absorption included, but the later is changed enough to explain the reduction of gap effects seen in the experiment. The principal difference between the absorption and no absorption bands is that the absorption effectively broadens the bands into the gaps. The band structure is modified back toward that of a free electron.^{5,6}

The band states of a crystal are produced by the interference of waves scattered by the regular array of atoms. The presence of inelastic scattering reduces the amplitude of waves reflected back from

greater distances, and therefore smooths out the finer features of the band structure just as replacing a large grating by two or three slits also broadens the diffraction features. Photoemission experiments share this feature with extended x-ray absorption fine-structure (EXAFS) experiments, which can be interpreted using a scattering by only the near neighbors rather than a treatment of the band structure.²¹ However, in EXAFS another feature of the experiment is also important in making this great simplification possible. In EXAFS the sharply localized source of waves is very near, or actually contained in the diffracting lattice. Thus the usual Fraunhofer diffraction common for gratings is replaced by what could be considered to be an extreme case of Fresnel diffraction, in which a wide variety of angles of incidence on the regular array of atoms occur together. This also blurs out the diffraction features. Thus in EXAFS a single-scattering approximation can be used profitably in the same energy range where a multiple-scattering treatment is absolutely required in LEED and in the usual photoemission, although such simplifications are also possible in photoemission from surface atoms.²² A free electron in an effective medium appears to give an interesting approximation for bulk photoemission (see below).

The upper-state bands with absorption should be used for determining k_z in the standard procedure for obtaining the initial-state bands from the angular photoemission experiment, rather than the usual bands without absorption. While $\text{Re}k_z$ remains zero in the gap for the ordinary band structure, we find that $\text{Re}k_z$ changes uniformly through the gap region at the same rate as it changes within the bands for either band structure.

The panel on the right in Fig. 4 shows κ , the imaginary part of k_z for the most important band in the left-hand panel. For no absorption, κ is zero within the bands but rises to a value of 0.17 \AA^{-1} on the real line in the gap which connects the bands at 15 and 24 eV. For $\beta=1.75$ eV, the value of κ in the bands is generally about 0.15 \AA^{-1} which increases to a value of 0.22 \AA^{-1} in the middle of this gap. The most reasonable definition of the mean free path, l , of an electron in a wave is the reciprocal of the decay exponent of the intensity of this wave, i.e., $l=1/(2\kappa)$. Thus, the most important Bloch wave in the final state has a mean free path of 3 \AA in the band and 2 \AA in the gap according to the calculations. The quantity l can be related to the lifetime, τ , of an electron in a band state by $l=v_g\tau$, where $v_g=\hbar^{-1}dE/dk$ is the group velocity, since, on the average, and electron will move a distance l

in the time before inelastic collision. The inverse lifetime expressed in energy units is thus $\hbar/\tau = l^{-1}dE/dk$. Combining this definition of τ with the approximate equation [(9)] gives $2\beta\tau \cong \hbar$, an approximate uncertainty relation between the lifetime and 2β , i.e., twice the imaginary contribution to the potential due to inelastic scattering. In Eq. (12), 2β is seen to be a peak width. Using the result for κ in the band and the slope of the band in Fig. 4, the lifetime is 1.7 eV, in reasonable agreement with the previously published¹ estimate of 2 eV. (This latter estimate should really be considered a determination of β which we also find to be 2 eV.)

A free-electron estimate of the decay length in the band can be obtained from the formula⁷

$$\frac{\hbar^2(k+i\kappa)^2}{2m} = E + i\beta, \quad (13)$$

where E is the energy measured from the bottom of the valence band. This equation is an approximation to Eq. (2). The imaginary part of this equation gives

$$\frac{\hbar^2 k \kappa}{m} = \beta, \quad (14)$$

which resembles the approximate equation [(9)]. Using the same value of β as in the band calculations, this equation gives a value of 4.4 Å for the mean free path l . This is somewhat different from the more accurate values obtained previously including band effects. We can explain this difference qualitatively by arguing that the electron must follow a curved path through the potential from one plane to the next which is longer by a factor of 1.5 over the direct free-electron motion without the potential. Thus Eq. (13) is not completely accurate for a non-free-electron material like nickel. It is reasonable to compensate for this factor by using an effective mass in both equations [(13) and (14)] over a limited energy range. This represents an electron moving through an effective medium.

VI. EFFECTS OF DAMPING IN THE INTERPRETATION OF EXPERIMENTAL DATA

Figure 5 shows the theoretically calculated (paramagnetic) lower band involved in the photoemission process, as a solid curve. Sections of the upper-state band (with absorption) are also shown, translated down by some of the photon energies, as dot (16 eV) and diamond (13 eV) lines, in such a

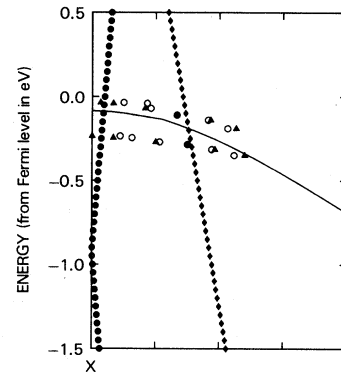


FIG. 5. Effect of the lifetime broadening on the experimental determination of $E(k)$. Triangles are $E(k)$ points determined without absorption, and the open circles are the same data interpreted using a final state with an absorption of 1.75 eV. Solid line is the calculated (paramagnetic) initial band. Solid circle and diamond lines are the final-state band calculated with this absorption shifted down by a 16 and 13 eV, respectively, so that the crossings of these lines with the initial bands indicates the energy and k_z for direct transitions in the data at these photon energies.

way that the conditions for direct transition, i.e., $k_z^f = k_z^i$ and $E^i = E^f - \hbar\nu$ are satisfied where these curves cross the solid curve representing the initial-state band. We might expect a significant change in the lower-state band structure obtained by using the bands with absorption rather than the usual upper-state bands in interpreting the experimental data shown in Fig. 1. Actually, the experimental points which were used in finding the lower bands lie outside, or at worst, on the border of the region where the upper-state curves are changed by absorption. Thus, using the final-state bands with absorption rather than the usual bands for interpreting the experiment gives very little change. The modification is shown in the figure as the change from the solid triangle points to the open circles. The same symbols are used for both the spin-up and spin-down bands.

The peaks remain stationary in energy for photons between 15 and 18 eV because the initial bands are very flat in a very small region around the X point. The photoemission in the gap is large because the initial density of states is high in this region. In this small region, the initial density of states actually seen in the experiment is modified by hole-lifetime effects which are not included in the present calculations. The effect is to reduce the effect of the high density of states in the narrow flat region by broadening the transition over a larger region in k_z .

VII. PHOTOEMISSION FROM COPPER

The amount of inelastic scattering of an electron in the upper state can be obtained much more directly from constant-initial-state measurements. The quantity ζ in Eq. (12) can be made small in comparison to β by choosing an initial state for which $\partial E/\partial k_z$ is large. When this can be done, constant-initial-energy experiments give a fairly direct determination of β , as the half-width at half-maximum for each direct-transition peak seen. In any case $\beta + \zeta$ can be determined. We shall compare this method of determination with the procedure of matching the experimental curves to theoretical curves calculated for various values of β . In Fig. 6 we show the experimental curves of Himpsel and Eberhardt² obtained in this mode along with theoretical curves calculated for various values of β . The large direct-transition peak around 84 eV in the experiment is reproduced excellently by theory, including a shoulder, for a value of β somewhere around 4 eV. A Lorentzian curve corresponding to Eq. (6b) with β equal to 5.0 eV is also shown for comparison. This gives the shape of the

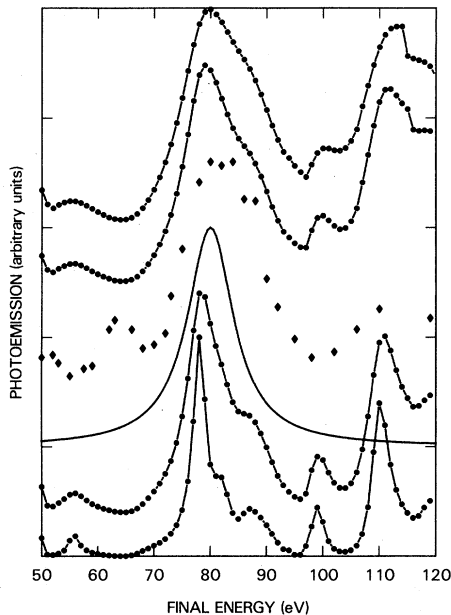


FIG. 6. Experimental and theoretical constant-initial-state spectra for normal emission from Cu(100) in the range from 50 to 200 eV. Diamond points are the experimentally determined values. Dots are theoretically determined values for various values of the absorption β : 1, 2.5, 4.0, and 5.0 eV going from the bottom to the top of the figure. Solid curve is a simple Lorentzian for $\beta=5.0$ eV placed below the experimental peak for comparison.

peak (without the shoulder) quite well. Note, however, that the estimate of β we obtain from the detailed calculations is somewhat smaller than one would obtain for a Lorentzian fit.

It is not possible to see the variation of β with energy from this data alone, since there is a strong direct transition at only one energy. There is also a small peak in the experiment at about 65 eV which is not reproduced by the theory. Similar emission has also been seen from Cu(110).²³ We find a final-state band in our calculation connected to the initial state by a direct transition at this energy, but the intensity calculated for it is too small to give a peak in this figure. The reason this peak is so small in the calculation is that this upper state is transmitted through the surface very poorly, probably because this flat band has little of the character of the plane wave it must match outside the crystal. This flat band should have a larger matrix element with the initial state, and a higher density of states, but these effects are not strong enough in the present calculation to make up for this poor transmission. Since this transition is excited by the component of the electric field perpendicular to the surface, field-enhancement effects⁴ in the surface of the crystal may be involved in producing the observed intensity in this peak. There are also sharp changes in the theoretical curves for large energy (115 eV) and large β which are probably artifacts of the calculation due to poor convergence of the beam expansion under these conditions.

Figure 7 shows a direct transition peak at 10.6 eV observed in normal emission from this same surface by Eastman, Knapp, and Himpsel.³ We also show calculations of this peak for assumed values of the damping β of 0.2, 0.4, and 0.6 eV. Our calculations determine a value of β of 0.4 eV, which is again less than the value 0.6 eV, that has been obtained by a simple Lorentzian fitting.³ The origin of this discrepancy is not clear. It is possible that the variation of bulk-cell matrix elements across the line discussed at the end of Sec. II plays a role. Combining the work on this 10.6-eV peak with the results for the 84-eV peak, two points on the absorption-versus-energy curve for the Cu(100) system are available at the present time. More data for Cu(110) is promised in Ref. 14 of Ref. 23.

Notice that the calculation peaks must be shifted by a few tenths of an eV to superimpose them on the experimental peak. This is perhaps at least partly explained by a real contribution to the potential from the self-energy which is different from the contribution to the ground state by an amount which is roughly equal to its imaginary contribution

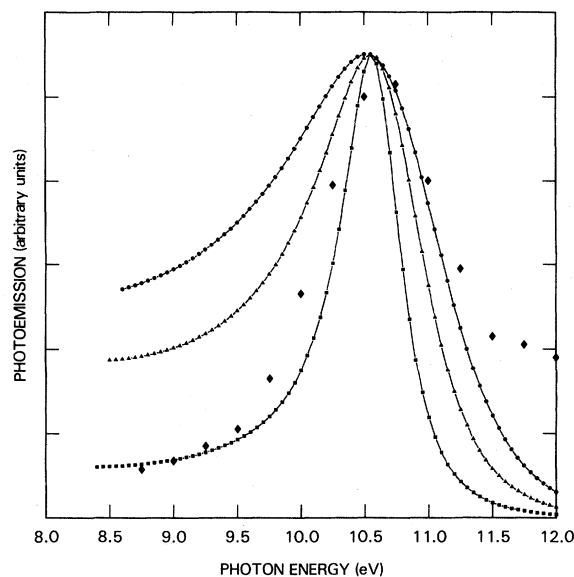


FIG. 7. Experimental and theoretical constant-initial-state spectra for normal emission from Cu(100) around 10 eV. Diamond points are the experimentally determined values. Lines drawn with various symbols are determined theoretically for values of the absorption β of 0.2, 0.4, and 0.6 eV, for the curves with squares, triangles, and dots, respectively. Calculated results have been arbitrarily shifted up in energy by 0.4, 0.5, and 0.6 eV, respectively, to match the peak positions to that of the experimental data (see text).

at this excitation energy. These real and imaginary parts are comparable in size in jellium calculations,¹³ and LEED determinations for nickel.²⁴

The experimental peak in Fig. 7 shows a small asymmetry in the form of a tail to higher energies. The theoretical curves also show such a tail, but on the low-energy side of the peak. The origin of the tail in the theoretical curves has been determined from an examination of intermediate results in the calculations, and can be stated in simple terms. In the neighborhood of the peak Eq. (2) can be written approximately as

$$I \propto \left| \frac{1}{\Delta k + i\kappa} + a + ib \right|^2, \quad (15)$$

where the first term in this absolute value represents the dominant term in the sums which is responsible for the direct transition and $a + ib$ represents the contribution from the sum of all of the other terms which remains relatively constant as the energy changes across the width of the peak. The first term has a pole near the real axis in the center of the peak, so that this term goes through a change in phase of 180° as the energy changes across the peak

profile. This means that the two terms under the absolute value sign will tend to add on one side of the peak and will tend to subtract on the other. This gives a modified line shape of the form

$$\frac{A + B\Delta E}{(\Delta E)^2 + \beta^2}. \quad (16)$$

Thus a direct transition is analogous to a resonant process in the theory of Fano,²⁵ and we obtain the usual Fano resonant line shape.

Closer analysis of the computer calculations shows that even more can be said. There are only two Bloch waves in the initial state which give important contributions to the formation of this peak shape. One of these waves is incident on the surface from inside the bulk of the crystal, and the other, moving back into the crystal from the surface, is produced from it by reflection from the surface. The reflected wave produces the first term in Eq. (15) and produces the direct transition, while the incident wave is responsible for most of the background term $a + ib$. The relative phase of these two terms, which determines whether constructive interference and hence the tail, will occur above or below the peak is fixed by the reflection at the surface. The theoretical calculation gives the tail on the wrong side of the peak because our model of the surface region apparently gives the relative phase of these two waves incorrectly.

The calculation has been repeated with a random-phase relation between these two waves, representing diffuse reflection at the surface, and with the phase artificially shifted by 180° . These results are plotted along with the original curve and the experimental curve in Fig. 8. We see that with the 180° phase change the tail of the experimental curve is reproduced somewhat better. The same change improved the agreement with experiment in previous work on copper.¹⁸

In very recent work, the curve with open squares was obtained by using a Lang-Kohn potential²⁶ suitable for copper to give the surface profile, rather than a hyperbolic tangent shape. This gives the large tail on the peak to the right without any adjustment of the phase. The curve shown here was obtained with a damping of 0.5 eV. This fits the experiment well around the center of the peak but has too small a tail to higher energy. We intend to extend this work to other choices of the surface potential.

The width chosen for the rise in the potential between the inside surface of the crystal and vacuum also had an effect on the shape of the photoemission curves for nickel. The curves shown in the fig-

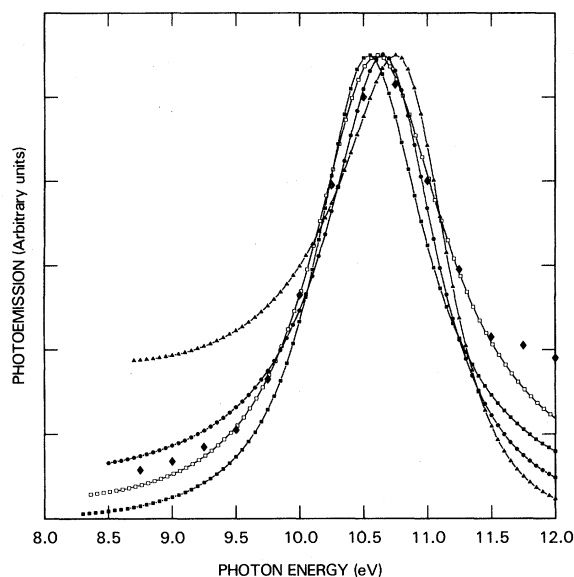


FIG. 8. Experimental and theoretical constant-initial-state spectra for normal emission from Cu(100) around 10 eV. Diamond points are the experimentally determined values. Lines with dots of various shapes are theoretically determined values obtained for various choices of the phase shift in the scattering of the Bloch waves in the initial state at the surface (see text). Curve drawn with triangles is the standard calculation for 0.4 eV shown in Fig. 7. Curve drawn with squares is the same calculation except that the phase difference between these waves has been changed by 180° . Curve drawn with dots was obtained by dropping the background Bloch wave, corresponding to diffuse scattering at the surface. Curve drawn with open squares was obtained by using a more realistic surface step potential (see text). Theoretical curves have been shifted so that the peak is at the same energy as that of the experimental curve.

ures were calculated for a very gradual transition with a width of about 1 \AA where this sensitivity is only minor. For a somewhat sharper transition of about 0.6 \AA , the photoemission, particularly at the X point, is reduced by interference within the initial state. Again, the contributions from the Bloch wave incident on the surface from within the crystal interferes with the contribution from the Bloch wave reflected back into the crystal from the surface. When this transition region was taken still narrower, about 0.3 \AA (which gives behavior approximating that of a sharp step), a surface resonance moved down from above the Fermi level to

the initial-state energies involved in these experiments. Since neither the interference effect nor the surface resonance are seen in the experimental results, we conclude that a gradual transition is a better description of the electron density profile in this nickel surface. It is clear that this scattering of Bloch waves by the surface in photoemission deserves more attention.

VIII. SUMMARY

Experimental data has been interpreted using calculated curves to estimate the inelastic scattering of an electron in the upper state. Comparison has been made with values obtained from simple peak-width formulas. Two types of experiments have been treated, experiments which give energy distribution curves at constant-photon-energy and constant-initial-state experiments. The second of these experiments is found to be easier to use for this purpose. The calculated elastic peak shapes for nickel are more complicated than those given by simple formulas, with tails to deeper energy which could be confused with inelastic contributions. However, half-widths at half maximum appear to be quite similar. In the Ni(110) data treated here, bulk emission occurs into what should be a gap in the band structure. Here the upper state calculated without lifetime effects has a gap, but including the inelastic scattering gives band lines across the gap in a narrow region of k which correspond to a modification of the band structure back toward the free-electron case. In this narrow region the initial-state band is very flat. This gives peaks which do not move with energy (like surface emission) over the region of the gap, in spite of the fact that they are clearly direct-transition peaks. Using the undamped final-state band instead of the band damped by inelastic scattering for an empirical determination of the initial-state bands leads to no significant error in the work previously reported for Ni(110) normal emission.

ACKNOWLEDGMENT

The first author would like to thank D. Spanjaard for discussions on some of the work described in this paper.

- ¹P. Heimann, F. J. Himpsel, and D. E. Eastman, *Solid State Commun.* **39**, 219 (1981).
- ²F. J. Himpsel and W. Eberhardt, *Solid State Commun.* **31**, 747 (1979).
- ³D. E. Eastman, J. A. Knapp, and F. J. Himpsel, *Phys. Rev. Lett.* **41**, 825 (1978); J. A. Knapp, F. J. Himpsel, and D. E. Eastman, *Phys. Rev. B* **19**, 4952 (1979).
- ⁴N. V. Smith, R. L. Benbow, and Z. Hurych, *Phys. Rev. B* **21**, 4331 (1980), and references cited in this paper.
- ⁵P. O. Nilsson and N. Dahlbäck, *Solid State Commun.* **29**, 303 (1979).
- ⁶See, in particular, J. Stohr, G. Apai, P. S. Wehner, F. R. McFeely, R. S. Williams, and D. A. Shirley, *Phys. Rev. B* **14**, 5144 (1976); P. O. Nilsson, J. Kanski, and C. G. Larsson, *Solid State Commun.* **36**, 111 (1980).
- ⁷J. C. Slater, *Phys. Rev.* **51**, 840 (1937).
- ⁸T.-C. Chiang, J. A. Knapp, D. E. Eastman, and M. Aono, *Solid State Commun.* **31**, 917 (1979).
- ⁹D. J. Spanjaard, D. W. Jepsen, and P. M. Marcus, *Phys. Rev. B* **15**, 1728 (1977).
- ¹⁰F. Jona, *J. Phys. C* **11**, 4271 (1978).
- ¹¹For such a treatment, see M. Baranger, *Phys. Rev.* **111**, 481 (1958); **111**, 494 (1958); **112**, 855 (1958).
- ¹²H. Kantor, *Phys. Rev. B* **1**, 2347 (1970); J. C. Tracy, *J. Vac. Sci. Technol.* **11**, 280 (1974); P. W. Palmberg and T. N. Rhodin, *J. Appl. Phys.* **39**, 2435 (1968).
- ¹³B. I. Lundqvist, *Phys. Status Solidi* **32**, 273 (1969).
- ¹⁴C. G. Larsson and J. B. Pendry, *J. Phys. C* **14**, 3089 (1981).
- ¹⁵Z. Hussain, E. Umbach, J. J. Barton, J. G. Tobin, and D. A. Shirley, *Phys. Rev. B* **25**, 672 (1982).
- ¹⁶P. J. Feibelman and D. E. Eastman, *Phys. Rev. B* **10**, 4932 (1974), Eq. (42); Ref. 9, Eq. (42); Actually the many-body theory of photoemission with a finite-hole lifetime contains other terms which do not contain this factor and therefore are not expected to peak at direct transitions. Apparently, their contributions are small.
- ¹⁷E. Dietz and F. J. Himpsel, *Solid State Commun.* **30**, 234 (1979).
- ¹⁸D. W. Jepsen, *Phys. Rev. B* **20**, 402 (1981).
- ¹⁹J. B. Pendry, *Low Energy Electron Diffraction* (Academic, New York, 1974); D. W. Jepsen and P. Marcus, in *Computational Methods in Band Theory*, edited by P. M. Marcus, J. F. Janak, and A. R. Williams (Plenum, New York, 1971).
- ²⁰V. L. Moruzzi, J. F. Janak, and A. R. Williams, *Calculated Electronic Properties of Metals* (Pergamon, New York, 1978), p. 95.
- ²¹C. A. Ashley and S. Doniach, *Phys. Rev. B* **11**, 1279 (1975); P. A. Lee and J. B. Pendry, *Phys. Rev. B* **11**, 2795 (1975).
- ²²D. H. Rosenblatt, J. G. Tobin, M. G. Mason, R. F. Davis, S. D. Kevan, D. A. Shirley, C. H. Li, and S. Y. Tong, *Phys. Rev. B* **23**, 3828 (1981).
- ²³P. Thiry, D. Chandesris, J. Lecante, C. Guillot, R. Pinchaux, and Y. Petroff, *Phys. Rev. Lett.* **43**, 82 (1979).
- ²⁴J. E. Demuth, P. M. Marcus, and D. W. Jepsen, *Phys. Rev.* **11**, 1460 (1975).
- ²⁵U. Fano, *Phys. Rev.* **124**, 1866 (1961).
- ²⁶N. D. Lang and W. Kohn, *Phys. Rev. B* **1**, 4555 (1970).